

Optimizing T_c in the (Mn,Cr,Ga)As and (Mn,Ga)(As,P) Ternary Alloys

J. L. Xu and M. van Schilfgaarde

*Department of Chemical and Materials Engineering,
Arizona State University, Tempe, AZ, 85287**

(Dated: March 23, 2022)

Abstract

We explore two possible ways to enhance the critical temperature T_c in the dilute magnetic semiconductor $\text{Mn}_{0.08}\text{Ga}_{0.92}\text{As}$. Within the context of the double-exchange and RKKY pictures, the ternary alloys $\text{Mn}_x\text{Cr}_{0.08-x}\text{Ga}_{0.92}\text{As}$ and $\text{Mn}_{0.08}\text{Ga}_{0.92}\text{As}_y\text{P}_{1-y}$ might be expected to have T_c higher than the pseudobinary $\text{Mn}_{0.08}\text{Ga}_{0.92}\text{As}$. To test whether the expectations from model pictures are confirmed, we employ linear response theory within the local-density approximation to search for theoretically higher critical temperatures in these ternary alloys. Our results show that neither co-doping Mn with Cr, nor alloying As with P improves T_c . Alloying with Cr is found to be deleterious to the T_c . $\text{Mn}_{0.08}\text{Ga}_{0.92}\text{As}_y\text{P}_{1-y}$ shows almost linear dependence of T_c on y .

PACS numbers: 75.50.Pp, 75.30.Et, 71.15.Mb

Searching for spintronic materials with high Curie temperature T_c has attracted a lot of interest recently^{1,2} because of the promising future of these materials. In spintronics technology, by including both magnetic and electronic properties in the devices, we can manipulate the electronic spin to the same degree as what we do to the electronic charge in conventional semiconductor devices. It can greatly improve the performance of current digital information processing and storage technology. Currently, one of the central issues for spintronics application is the development of carrier-mediated ferromagnetic semiconductors that are magnetic above room temperature. Dilute magnetic semiconductors (DMS), i.e. semiconductors doped with low concentrations of magnetic impurities (such as Mn, Co, Cr), are generally thought to be good candidates for these spintronics applications. $\text{Ga}_{1-x}\text{Mn}_x\text{As}$ is one of the most widely studied DMS, because it is one of the few materials where it is generally agreed that the magnetism is carrier-mediated.

Currently, much effort has been expended to increase T_c in $\text{Ga}_{1-x}\text{Mn}_x\text{As}$ and related DMS materials. T_c has risen steadily in $\text{Ga}_{1-x}\text{Mn}_x\text{As}$, to $T_c \sim 180\text{K}$ in very thin films, carefully annealed to eliminate Mn interstitials without at the same time allowing MnAs precipitates to form^{3,4,5}. However, there is still a large gap between the highest T_c obtained to date and a technologically useful working temperature.

A systematic understanding of the ferromagnetism in DMS systems is necessary for the design and optimization of the materials. However, the theoretical understanding of this system is still not very clear, although several models were proposed. One generally used model is based on the assumption that Mn local magnetic moments interact with each other via RKKY-type interactions, the Mn at the same time providing a source of free holes⁶. This picture can explain the temperature dependence of the magnetization and the hole resistivity of the DMS, although there is a growing consensus that many of the claims of that paper were artifacts of the assumptions in the model. On the other hand, Akai⁷ first used the local spin-density approximation (LSDA) to estimate T_c within the Coherent Potential Approximation (CPA) in (In,Mn)As; he argued that a double exchange mechanism was a more appropriate description of the magnetism than the pd exchange assumed by Dietl.

In addition, there is a fair amount of research that indicates the ferromagnetism in DMS systems are strongly affected by the inherent disorder. In our recent work⁸ we included various effects of disorder, and found that there is a rather strict upper limit of around 250K for T_c in disordered Mn:GaAs systems (as computed within the LDA), which implies a rather

unpromising future for the simple Mn:GaAs alloy. So, it is becoming an important issue to find possible ways to optimize the magnetic properties of DMS. The possible means may include co-doping the magnetic elements, change of host materials and magnetic elements, or spacial confinement of the magnetic dopants, etc. We use the Zener double-exchange picture for guidance, for reasons that will be clear below. For detailed analysis we employ to the same LDA linear response techniques as in Ref.⁸.

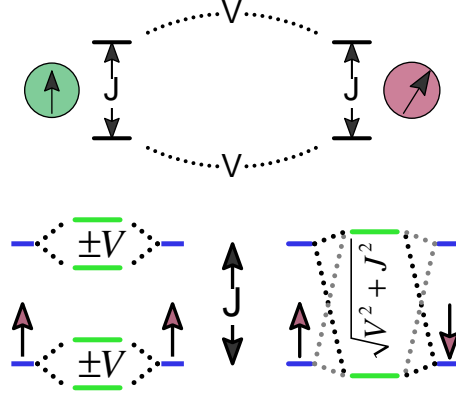


FIG. 1: Cartoon of the Zener model coupling levels on two neighboring sites. Top illustrates the majority and minority levels on each site together with the model parameters (intra-atomic exchange splitting J , effective interatomic hopping matrix element V , and canting angle θ). Bottom left depicts the four levels when spins are aligned parallel; bottom right depicts the levels when spins are aligned antiparallel.

Here we consider two strategies to make alloys related to $\text{Mn}_x\text{Ga}_{1-x}\text{As}$, that can have higher T_c . We based both strategies on the double exchange/superexchange picture⁹ depicted in Fig. 1. The four levels are described by the hamiltonian

$$H = U^\dagger \begin{pmatrix} +J & 0 & V & 0 \\ 0 & -J & 0 & V \\ V & 0 & +J & 0 \\ 0 & V & 0 & -J \end{pmatrix} U, \quad (1)$$

with U the spinor rotation matrix for the second site:

$$U = \begin{pmatrix} 1 & 0 \\ 0 & U_2 \end{pmatrix}, \quad U_2 = \begin{pmatrix} \cos \theta/2 & -\sin \theta/2 \\ \sin \theta/2 & \cos \theta/2 \end{pmatrix} \quad (2)$$

The eigenvalues are given by the quartic equation⁹

$$\epsilon^2 = J^2 + V^2 \pm 2VJ \cos(\theta/2). \quad (3)$$

When only the lowest state is filled, the parallel alignment dominates (Zener double exchange). The most salient other characteristic of the Zener double exchange energy is its unusual non-Heisenberg dependence on angle, varying as $|\cos(\theta/2)|$. When the first two states are filled the energy vanishes for parallel spin alignment, and the system is stabilized in the AFM alignment (Anderson superexchange), the energy varying as $-\cos(\theta)$. As a function of filling, there is a transition from FM stabilization to AFM. The maximum FM stabilization occurs at half-filling.

In the $\text{Mn}_x\text{Ga}_{1-x}\text{As}$ and $\text{Cr}_x\text{Ga}_{1-x}\text{As}$ alloys, the exchange is mediated by the partially filled TM-derived t_2 impurity band. In the dilute limit, the Mn-derived t_2 level has threefold degeneracy and falls at VBM+0.1 eV, while the Cr-derived level falls at VBM+0.3 eV. These levels broaden into an impurity band as x increases. In reality this band is composed of an admixture of TM d states and effective-mass like states of the host^{10,11}, mostly derived from the top of the host valence band.

To the extent that the model correctly describes exchange in $\text{Mn}_x\text{Ga}_{1-x}\text{As}$, it is possible to optimize T_c of a specific DMS system by varying the carrier concentration to set this impurity band as close to half filling as possible. One possible way to do this is to make a pseudoternary alloy $\text{Mn}_x\text{Cr}_y\text{Ga}_{1-x-y}\text{As}$, where the (Mn,Cr,Ga) atoms share a common (fcc) sublattice. Cr has one electron to fill the 3-fold majority t_2 level to 1/3 filling. Mn has two electrons, so the majority t_2 level should be 2/3 full. By alloying Mn and Cr, we might obtain a compromise 1/2 filling that will increase T_c .

Another possibility is to vary the anion in the III-V series. From model viewpoints (and confirmed by the LDA), there are two competing effects from the anion. The important quantity is the position of the transition-metal d level relative to the top of the valence band (determined largely by the anion p level). When the anion is heavy (e.g. Sb) the p is shallow; the Mn d sits mostly below the valence band, and the t_2 derived impurity band is mostly composed of the effective-mass like host states; thus the exchange is effectively mediated the holes near the valence band top, as the RKKY picture assumes. If the Mn d is very deep, the coupling between the Mn and holes also weak, so the interatomic exchange is small. As the anion becomes lighter (Sb→As→P→N) the anion p deepens, so that finally

the Mn d falls above the valence band and forms a deep level. In this limit the coupling should be well described by double-exchange. For Mn in GaN, the t_2 level is approximately at midgap. It couples strongly to nearest neighbors, but is short ranged. At least in the dilute case, the near-neighbor exchange interactions are mostly ferromagnetic and rather strong, but they decay rapidly with distance⁸. But also in the dilute case, there are few nearest neighbors and more distant interactions are necessary for long-range order to exist, as without them there is no percolation path. The net result is that T_c is predicted to be quite low in $\text{Mn}_x\text{Ga}_{1-x}\text{N}$ ¹². The anion with the highest T_c will adopt some compromise between a very deep valence band (GaN) and a very shallow one (GaSb). With this picture, and the expectation that the Mn d level in MnGaP is perhaps already too high, we might be able to make a ternary $\text{MnGaP}_x\text{As}_{1-x}$ where x can be adjusted to tune the position of the valence band, and thus optimize T_c .

First principles calculations provide a way for evaluation of the exchange interactions and T_c in a DMS system of a specific geometry. We adopt here the same scheme as presented in Ref.⁸, to study the ferromagnetic trends for the ternaries $\text{Mn}_x\text{Cr}_{0.08-x}\text{Ga}_{0.92}\text{As}$ and $\text{Mn}_{0.08}\text{GaP}_y\text{As}_{1-y}$. Self-consistent calculations of 200-atom special quasirandom structures¹³, or SQS, were performed using the method of Linear-Muffin-Tin Orbitals (LMTO) within the local spin density approximation (LSDA) and the Atomic Spheres Approximation^{14,15}. The exchange interactions were computed within the long-wave approximation using a linear response Green's function technique, which maps the total energy onto a Heisenberg form. The interatomic Heisenberg exchange parameters are determined from the linear response expression

$$J_{ij}^\perp = \frac{1}{2\pi} \int^{\varepsilon_F} d\varepsilon \text{ImTr}_L \left\{ P_i \cdot \left(T_{ij}^\uparrow \cdot T_{ji}^\downarrow + T_{ij}^\downarrow \cdot T_{ji}^\uparrow \right) \cdot P_j \right\} \quad (4)$$

where i and j are indexes of atoms with the on-site perturbation having a form $P = P_Z = (T_\uparrow^{-1} - T_\downarrow^{-1})/2 = (P^\uparrow - P^\downarrow)/2$, as described in Ref.¹⁵. P is a diagonal matrix whose rows and columns correspond to the orbitals at a particular site (*spd* in the present case); P is closely related to the majority-minority spin-splitting. $T_{ij}^\uparrow \cdot T_{ji}^\downarrow$ essentially the transverse susceptibility. Magnetization at finite temperature and T_c were calculated using the Cluster Variation Method (CVM) of Kikuchi¹⁶, generalized to the continuous rotational degrees of freedom of the (classical) Heisenberg model, which predicts T_c to within about 5% of results calculated by full spin-dynamics simulations in these DMS alloys⁸. For both $\text{Ga}_{0.92}\text{Mn}_{0.08}\text{As}$ and $\text{Ga}_{0.92}\text{Cr}_{0.08}\text{As}$ the CVM predicts T_c of about 280K. We will show that, although these

two systems are intriguing based on the simple pictures we carry around about them, neither alloy is predicted to have magnetic properties more favorable than $\text{Mn}_x\text{Ga}_{1-x}\text{As}$ at $x = 0.08$.

Before addressing T_c in the pseudoternary $\text{Mn}_x\text{Cr}_y\text{Ga}_{1-x-y}\text{As}$, we consider a simple model calculation to see to what extent the LDA exchange interactions approximately parallel the double-exchange picture. Starting from $\text{Mn}_{0.08}\text{Ga}_{0.92}\text{As}$ SQS configuration, we artificially shift the Fermi level of this system to mimic additional doping. In this model dopant electrons are assumed to have no effect but change the filling of the valence band, which enables us to isolate this effect from other complexities that occur in the real system, but which are missing in the double-exchange model.

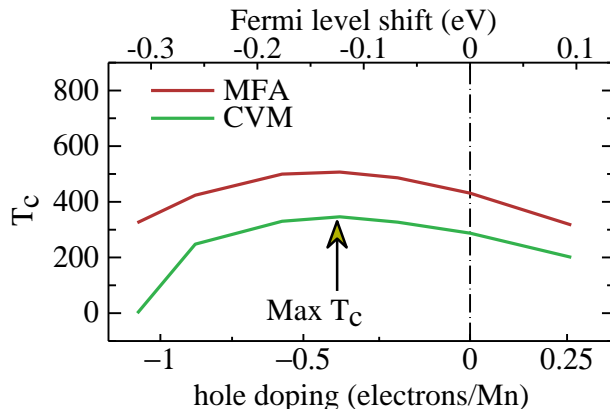


FIG. 2: Dependence of T_c Fermi level shift and the corresponding change in band occupancy. Calculated MFA and CVM T_c are presented as a function of Fermi level shift and deviation from charge neutrality.

Fig. 2 shows the change in T_c due to the Fermi level shift ΔE_F (and corresponding hole doping), in a 200-atom SQS structure $\text{Ga}_{92}\text{Mn}_8\text{As}_{100}$. As predicted by both the RKKY picture and the double-exchange picture, increasing E_F reduces the number of holes and reduces T_c . Conversely, with the initial introduction of more holes ($\Delta E_F < 0$) T_c increases as both RKKY picture and double-exchange models predict. However, fig. 2 shows that T_c reaches a maximum for $\Delta E_F \sim -0.20$ eV; further shifts reduce T_c . Observing the Fermi level shifts in the DOS we can confirm that position of E_F at optimum T_c corresponds to E_F falling in the middle of the Mn t_2 band, indicating half filling of the t_2 level. This can be determined independently by counting the number of holes added as a function of ΔE_F . $\Delta E_F \sim -0.20$ eV corresponds to the addition of approximately 4 holes in this system of 8 Mn atoms, or 0.5 hole/atom. The t_2 level with initially 2 electrons ($\Delta E_F = 0$) changes

to 1.5 electrons near $\Delta E_F = -0.2$, which is just half of the number needed to fill the level. This confirms that the double-exchange picture more closely reflects the *ab initio* LDA calculations than does RKKY, as Akai first proposed⁷.

One possible way to introduce holes in a real system is to add another dopant, e.g. Be, as has been done in δ -doped MnGaAs¹⁷. However, Be doping appears to catalyze the formation of other deleterious defects (probably Mn interstitials, which being donors, bind to Be). Another way is to alloy Cr with Mn. In the simplest view we can mimic this effect by a “virtual crystal” where we use a hypothetical atom X with atomic number 24.5. The T_c evaluated for this hypothetical $\text{Ga}_{92}\text{X}_8\text{As}_{100}$ SQS structure is dramatically larger than T_c for $\text{Ga}_{92}\text{Mn}_8\text{As}_{100}$ or $\text{Ga}_{92}\text{Cr}_8\text{As}_{100}$, as we found before. For this 8% doping case, the T_c is calculated to be 710K with the MFA and 390K within the more reliable CVM.

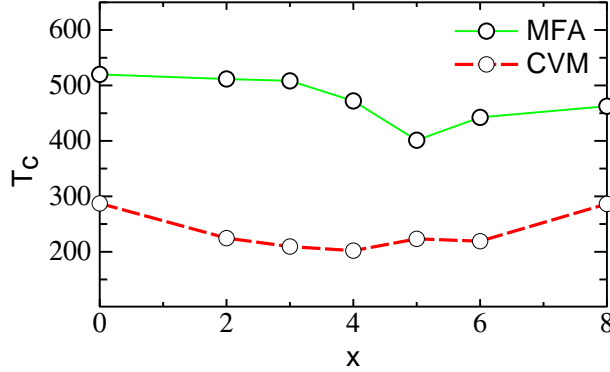


FIG. 3: Dependence of T_c on y in $\text{Mn}_x\text{Cr}_y\text{Ga}_{1-x-y}\text{As}$. T_c is computed both within the MFA and the CVM. The noise in the data occurs because T_c depends on the specific choice of quasi random configuration. For the same y , there can be a deviation between different SQS structures as much as 50K.

Finally, we consider a physically realizable configuration, $\text{Mn}_x\text{Cr}_y\text{Ga}_{1-x-y}\text{As}$. We now construct a series of three-body 200-atom SQS structures, varying x for fixed $x + y = 8\%$. T_c was calculated for all a variety of configurations with different x . The calculated Curie temperature depending on x are shown in Fig. 3. The picture that emerges is, unfortunately very different from the virtual crystal. Co-doping actually decreases T_c . We can see although CVM and MFA T_c curves have a little different shape, they both predict T_c to decrease near $x = 1/2$, in contradistinction to the virtual crystal. The reason can be traced to the fact that Cr and Mn have their impurity levels at different energies. Consider the limit of infinitely narrow impurity bands: there is a Cr-derived level at VBM+0.3 eV and a Mn-derived level

at VBM+0.1 eV. The single electron in the Cr-derived level falls to the Mn level, thus emptying out the Cr t_2 state and completely filling the Mn t_2 state. In the double-exchange picture, the system will be antiferromagnetic. In the alloy, these levels broaden into bands. However the Mn and Cr like states derive from sufficiently different energies, so that rather than forming a single wide impurity band made of equal admixtures of Cr and Mn, the band is composed of a lower part more of Mn character and an upper part dominated by Cr. If the bandwidth is not sufficiently large to counter this effect, the net result is that $T_c(x)$ in the true ternary apparently bows oppositely to what occurs in the idealized case.

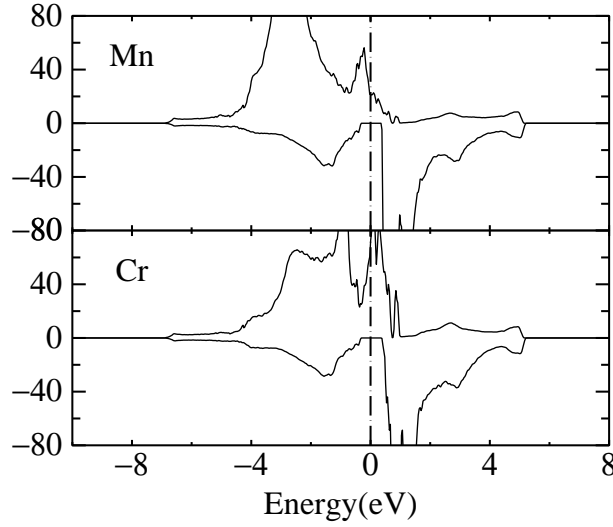


FIG. 4: Energy resolved Partial DOS of Mn and Cr ions in $\text{Ga}_{92}\text{Mn}_4\text{Cr}_4\text{As}_{100}$, showing similar filling as single element doping case.

This is reflected in the partial DOS of TM in (Mn,Cr):GaAs(Fig. 4). The DOS of the t_2 for each individual TM ion reflects the DOS in the respective pseudobinary alloy: the Mn t_2 near E_F is centered slightly below the Cr t_2 , showing the localized behavior of magnetic dopants. Some broadening is evident (particularly in the tail of the Mn t_2 above E_F , but owing to the dilute alloy concentration the coupling between t_2 levels is not sufficient to broaden it into a homogeneous band. The lack of this distinction makes the virtual crystal approximation an unsuitable description of the real alloy. When both levels are present the deeper Mn t_2 (2/3 full in Mn:GaAs) becomes fuller still, while the Cr t_2 (1/3 full in Cr:GaAs) becomes more empty. Hence, the co-doping actually drive the filling opposite to the desired direction. The band is actually adversely affected, resulting in a decrease in T_c by co-doping.

It is notable that an RKKY-like picture⁶, which describes exchange interactions purely in terms of spin-split host bands whose splitting is determined by the local magnetic moments, will also miss this effect. This establishes in another way the fact that exchange interactions within the LDA more closely reflect the Zener double-exchange model than an RKKY-like model.

Our other strategy to increase T_c is to consider the ternary $\text{Mn}_{0.08}\text{Ga}_{0.92}\text{As}_y\text{P}_{1-y}$, as we described above. In this calculation, SQS configurations are also generated through independent sublattices of cations (Mn,Ga) and anions (As,P). the Mn concentration is fixed to be 0.08% as before. T_c for different P concentrations are studied. For the lattice constant, we use virtual crystal approximation with modification based on Ref.¹⁸. The figure shows that the net effect (deviation from linear behavior) is small. but in any case T_c bows downward with y , with T_c suppressed by $\sim 50\text{K}$ for $y = 0.5$. This reduction can be understood as a suppression, through disorder, of the number of paths that connect different magnetic sites, and thus the magnetic exchange between them.

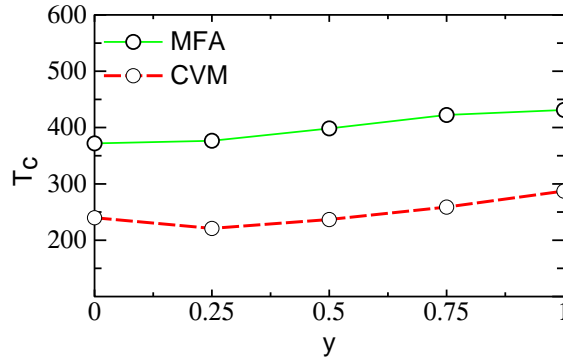


FIG. 5: Curie Temperature for $\text{Mn}_{0.08}\text{Ga}_{0.92}\text{As}_y\text{P}_{1-y}$ as a function of y

In conclusion, based on the LSDA, we found out the Curie Temperature of DMS can be improved by modifying the band filling, as both double exchange and RKKY models predict. We show that the LSDA results more closely parallel the double exchange than the RKKY picture, and predict that optimal T_c occurs when the impurity t_2 band is half full. However, when we attempt to modify the concentration in a real crystal like Mn and Cr co-doping GaAs, T_c is actually suppressed. For a successful application of this rule, it will be necessary to find another way to tailor the band occupancy in order to achieve half filling. We also found that admixing of As and P on the anion sublattice does not improve T_c .

This work was supported by the Office of Naval Research.

* Mark.vanSchilfgaarde@asu.edu

- ¹ H. Ohno, A. Shen, F. Matsukura, A. Oiwa, A. Endo, S. Katsumoto, and Y. Iye, *Applied Physics Letters* **69**, 363 (1996).
- ² Y. Ohno, D. K. Young, B. Beschoten, F. Matsukura, H. Ohno, and D. D. Awschalom, *Nature* **402**, 790 (1999).
- ³ D. Chiba, K. Takamura, F. Matsukura, and H. Ohno, *Appl. Phys. Lett.* **82**, 3020 (2003).
- ⁴ K. C. Ku, S. J. Potashnik, R. F. Wang, S. H. Chun, P. Schiffer, N. Samarth, M. J. Seong, A. Mascarenhas, E. Johnston-Halperin, R. C. Myers, et al., *Appl. Phys. Lett.* **82**, 2302 (2003).
- ⁵ K. W. Edmonds, P. Bogusawski, K. Y. Wang, R. P. Campion, S. N. Novikov, N. R. S. Farley, B. L. Gallagher, C. T. Foxon, M. Sawicki, T. Dietl, et al., *Phys. Rev. Lett.* **92**, 037201 (2004).
- ⁶ T. Dietl, H. Ohno, F. Matsukura, J. Cibert, and D. Ferrand, *Science* **287**, 1019 (2002).
- ⁷ H. Akai, *Phys. Rev. Lett.* **81**, 3002 (1998).
- ⁸ J. L. Xu, M. van Schilfgaarde, and G. D. Samolyuk, *Phys. Rev. Lett.* **94**, 097201 (2005).
- ⁹ P. W. Anderson and H. Hasegawa, *Phys. Rev.* **100**, 675 (1955).
- ¹⁰ M. van Schilfgaarde and O. Mryasov, *Phys. Rev. B* **63**, 233205 (2001).
- ¹¹ P. Mahadevan and A. Zunger, *Phys. Rev. B* **69**, 115211 (2004).
- ¹² K. Sato, W. Schweika, P. H. Dederichs, and H. Katayama-Yoshida, *Phys. Rev. B* **70**, 201202(R) (2004).
- ¹³ A. Zunger, S.-H. Wei, L. G. Ferreira, and J. E. Bernard, *Phys. Rev. Lett.* **65**, 353 (1990).
- ¹⁴ A. I. Liechtenstein, M. I. Katsnelson, V. P. Antropov, and V. A. Gubanov, *J. Magn. Magn. Mater.* **67**, 65 (1987).
- ¹⁵ M. van Schilfgaarde and V. P. Antropov, *J. Appl. Phys.* **85**, 4827 (1999).
- ¹⁶ R. Kikuchi, *Phys. Rev.* **81**, 988 (1951).
- ¹⁷ T. Wojtowicz, W. L. Lim, X. Liu, M. Dobrowolska, J. K. Furdyna, K. M. Yu, W. Walukiewicz, I. Vurgaftman, and J. R. Meyer, *Appl. Phys. Lett.* **83**, 4220 (2003).
- ¹⁸ C. K. Shih, W. E. Spicer, W. A. Harrison, and A. Sher, *Phys. Rev. B* **31**, 1139 (1985).